Int. J. Heat Mass Transfer. Vol. 32, No. 11, pp. 2015–2025, 1989
Printed in Great Britain

0017-9310/89 \$3.00+0.00

Study of heat and mass transfer in a chemical moving bed reactor for gasification of carbon using an external radiative source

A. BELGHIT and M. DAGUENET

Laboratoire de Thermodynamique et Energétique, Université de Perpignan, Avenue de Villeneuve, 66025 Perpignan Cedex, France

(*Received* 18 *February* 1988 *and in final form* 17 *November* 1988)

Abstract—A theoretical model of a chemical moving bed reactor for gasifying carbon with CO_2 using an external radiative source (concentrated solar radiation) is proposed. It permits the determination of the temperature profile for gas and solid and the concentration profile in the gas as a function of control parameters: gas flow rate, warm surface temperature, diameter of particles. Comparison of model results with experiment gives satisfactory agreement.

1. INTRODUCTION

VARIOUS technical approaches use coal for conversion to gaseous and liquid fuels. The energy necessary to drive endothermic coal gasification reactions can be supplied by partial coal combustion, by preheating the reactant gas, or from an external radiative source, such as the sun.

The use of high-temperature solar energy to drive the endothermic reactions associated with coal and other carbonaceous materials for gasification has been studied by several investigators [1–5].

Recently, a moving bed reactor, shown in Fig. 1, for gasifying coconut charcoal (it is nearly pure carbon: 1.5 ± 0.5 wt% H with a low ash content of 1.2 wt%) with CO_2 was studied experimentally [6]. Experiments were carried out on a vertical solar furnace located at the C.N.R.S. Laboratory in Odeillo, France.

These tests were made with incident solar intensities ϕ_i of 290–690 kW m^{-2}, temperatures T_0 of 900–1200°C, gas flow rates F_{CO_2} of 1–11 l min^{-1} and particles with a diameter of 0.32 cm.

The performance of the reactor was defined on the

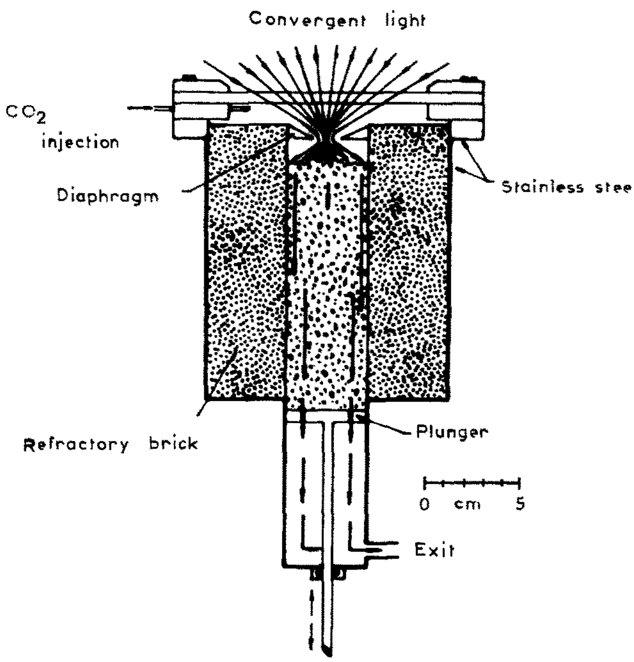

FIG. 1. Reactor used for solar gasification. As the packed bed was consumed it was pushed toward the focal plane.

NOMENCLATURE

A	(particle surface area)/(unit bed volume) [m^{-1}]
C	mass fraction of CO_2 in the gas mixture
c_p	heat capacity [$J\,kg^{-1}\,K^{-1}$]
d	particle diameter [m]
D	diffusion coefficient of CO_2 in the gas [$m^2\,s^{-1}$]
D_0	diameter of the cylinder containing the porous medium [m]
F_{CO_2}	CO_2 flow rate at the entry of the reactor [$m\,s^{-1}$]
h	particle–fluid heat transfer coefficient [$W\,m^{-2}\,K^{-1}$]
ΔH	molar enthalpy of reaction [$J\,mol^{-1}$]
K	extinction coefficient [m^{-1}]
k_g	mass transfer coefficient [$m\,s^{-1}$]
L	length of the packed bed [m]
M	molar density [$kg\,mol^{-1}$]
p	pressure inside the reactor [Pa]
q_r	radiation flux density in the solid
T	temperature of the solid [K]
v	fluid velocity [$m\,s^{-1}$]
V	volume of the packed bed [m^3]
v_s	solid velocity [$m\,s^{-1}$]
x	axial coordinate (positive in the flow direction) [m]
X	degree of advancement of reaction.

Greek symbols

ε	bed void fraction
η	thermochemical efficiency of the process
θ	gas temperature [K]
λ	thermal conductivity [$W\,m^{-1}\,K^{-1}$]
μ	viscosity [$N\,s\,m^{-2}$]
ρ	density [$kg\,m^{-3}$]
σ	Stefan–Boltzmann constant [$W\,m^{-2}\,K^{-4}$]
ϕ_i	incident radiative flux [$W\,m^{-2}$].

Dimensionless variables

Nu	Nusselt number, hd/λ
Pr	Prandtl number, $\mu c_p/\lambda$
Re	Reynolds number, $v_0 d\rho/\mu$
Sc	Schmidt number, $\mu/\rho D$
Sh	Sherwood number, $k_g d/D$
X^+	dimensionless axial coordinate, x/d.

Subscripts

a	ambient conditions
C	carbon
cal	calculated value
meas	measured value
p	particle
s	solid, superficial
0	reference value.

basis of the amount of solar energy stored (efficiency of the process, η) and the fraction of reactant gas consumed. The efficiency can be determined from the fuel value (heat of combustion) of the product gas (ΔH_p), the heat of combustion of the fuel gasified (ΔH_F) and the solar energy (ΔH_s) used during gasification as follows:

$$\eta = \left(\frac{\Delta H_p - \Delta H_F}{\Delta H_s}\right) \times 100.$$

In the above tests, the maximum of the fraction of reactant gas (CO_2) consumed was found to be 98% for $F_{CO_2} = 4$ l min^{-1} and $T_0 = 1150°C$, and the maximum efficiency was found to be 50% for $F_{CO_2} = 8.2$ l min^{-1} and $T_0 = 950°C$.

A major parameter in the study of transfer in this reactor is the overall rate of gasification, which is determined by a chemical, mass transport or mixed control, depending on experimental conditions.

A gravimetric analysis has determined a control of the reaction process by mass transport (diffusion through the gas film around a solid particle) for temperatures above 1000°C.

In addition to this work, a theoretical model of the functioning of the moving bed reactor with mass transport control is presented here.

2. HEAT AND MASS TRANSFER EQUATIONS

The reactor is assumed to be composed of a stacking of identical non-porous carbon grains regularly distributed in a drum. Its section is large enough that its sides may be considered as adiabatic; the flow is one-dimensional and the physical properties are the same for all points located in the same section.

Compared to other exchange modes (conduction, radiation and convection), viscous friction and pressure drops are considered as negligible. The flow is assumed to be steady and the gas flow rate constant. Heat and mass transfer equations are [6]:

for the gas

$$\rho v \frac{\partial C}{\partial x} = \frac{\partial}{\partial x}\left(\rho D \frac{\partial C}{\partial x}\right) + \sigma_C \quad (1)$$

$$\rho c_p v \frac{\partial \theta}{\partial x} = \frac{\partial}{\partial x}\left(\lambda \frac{\partial \theta}{\partial x}\right) + \sigma_\theta; \quad (2)$$

for the solid

$$-\rho_s \frac{\partial v_s}{\partial x} + \sigma_s = 0 \quad (3)$$

$$\rho_s c_{ps} v_s \frac{\partial T}{\partial x} = \frac{\partial}{\partial x}\left(\lambda_s^* \frac{\partial T}{\partial x}\right) - \frac{\partial q_r(x)}{\partial x} + \sigma_T. \quad (4)$$

In these equations, the terms σ_C, σ_θ, σ_s and σ_T represent mass or heat production in the control volume. They may be expressed as

$$\sigma_C = -\frac{A}{\varepsilon} k_g \rho (C - C_s)$$

$$\sigma_\theta = \frac{A}{\varepsilon} h (T_s - \theta)$$

$$\sigma_s = -\frac{A}{1-\varepsilon} \rho k_g (C - C_s)$$

$$\sigma_T = -\frac{A}{1-\varepsilon} h (T_s - \theta) - \frac{A}{1-\varepsilon} \Delta H k_g \rho (C - C_s).$$

In this case, the contact surface ratio may be written as

$$A = \frac{6(1-\varepsilon)}{d}.$$

The assumption of the existence of mass transport control around a grain allows the condition $C_s = C_e$, where C_e is determined by the chemical equilibrium reaction [7]. The thermal gradient is in the particle external boundary layer, where T_s is considered to be equal to T [8].

To simplify the study, the porous bed is assumed to be a gray optically thick medium characterized by extinction coefficient K and emissivity ε_p. The radiative flux density is given by [9]

$$q_r(x) = -\frac{16\sigma T^3}{3K} \frac{\partial T}{\partial x}$$

therefore

$$\frac{\partial q_r(x)}{\partial x} = -\left\{\frac{16\sigma T^2}{K}\left(\frac{\partial T}{\partial x}\right)^2 + \frac{16\sigma T^3}{3K}\frac{\partial^2 T}{\partial x^2}\right\}.$$

The set of equations (1)–(4) may be written as

$$\rho v \frac{\partial C}{\partial x} = \frac{\partial}{\partial x}\left(\rho D \frac{\partial C}{\partial x}\right) + \frac{6(1-\varepsilon)}{\varepsilon d} k_g \rho (C_s - C) \quad (5)$$

$$\rho c_p v \frac{\partial \theta}{\partial x} = \frac{\partial}{\partial x}\left(\lambda \frac{\partial \theta}{\partial x}\right) + \frac{6(1-\varepsilon)}{\varepsilon d} h (T - \theta) \quad (6)$$

$$\rho_s \frac{\partial v_s}{\partial x} = \frac{6}{d} \rho k_g (C_s - C) \quad (7)$$

$$\rho_s c_{ps} v_s \frac{\partial T}{\partial x} = \frac{\partial}{\partial x}\left[\lambda_s^* \frac{\partial T}{\partial x}\right] + \frac{16\sigma T^2}{K}\left(\frac{\partial T}{\partial x}\right)^2 + \frac{16\sigma T^3}{3K}\frac{\partial^2 T}{\partial x^2} - \frac{6}{d} h (T - \theta) + \frac{6}{d} \Delta H k_g \rho (C_s - C). \quad (8)$$

These equations are fitted with the following boundary conditions:

at $x = 0$: $T = T_0$, $\theta = \theta_0 = \theta_a$, $C = 1$, $v_s = 0$

at $x = L$: $\overrightarrow{\mathrm{grad}}_L\, \theta = 0$; $\overrightarrow{\mathrm{grad}}_L\, T = 0$; $\overrightarrow{\mathrm{grad}}_L\, C = 0$.

The numerical solution requires a certain dimensionless form of these equations and boundary conditions. Assuming that

$$X^+ = \frac{x}{d}, \quad T^+ = \frac{T}{T_0} \quad \text{and} \quad \theta^+ = \frac{\theta}{T_0}$$

the set of equations (5)–(8) can be written as

$$\frac{Re\, Sc}{\varepsilon} \rho D \frac{\partial C}{\partial X^+} = \frac{\partial}{\partial X^+}\left(\rho D \frac{\partial C}{\partial X^+}\right) + \frac{6(1-\varepsilon)}{\varepsilon} Sh\, \rho D (C_s - C) \quad (9)$$

$$\frac{Re\, Pr}{\varepsilon} \lambda \frac{\partial \theta^+}{\partial X^+} = \frac{\partial}{\partial X^+}\left(\lambda \frac{\partial \theta^+}{\partial X^+}\right) + \frac{6(1-\varepsilon)}{\varepsilon} Nu\, \lambda (T^+ - \theta^+) \quad (10)$$

$$\rho_s \frac{\partial v_s}{\partial X^+} = 6\rho \frac{Sh\, D}{d}(C_s - C) \quad (11)$$

$$\frac{\partial}{\partial X^+}\left[\left(\lambda_s^* B + \frac{T^{+3}}{3}\right)\frac{\partial T^+}{\partial X^+}\right] = 6\, Nu\, \lambda B (T^+ - \theta^+) - \frac{6\Delta H\, Sh\, D B \rho}{T_0}(C_s - C) + \rho_s c_{ps} v_s B d \frac{\partial T^+}{\partial X^+} \quad (12)$$

where $B = K/16\sigma T_0^3$ and the following boundary conditions apply:

at $X^+ = 0$: $T^+ = 1$; $\theta^+ = \dfrac{\theta_0}{T_0}$; $C = 1$; $v_s = 0$

at $X^+ = \dfrac{L}{d} = L^+$: $\dfrac{\partial T^+}{\partial X^+} = 0$; $\dfrac{\partial \theta^+}{\partial X^+} = 0$; $\dfrac{\partial C}{\partial X^+} = 0$.

3. PARAMETERS

Heat and mass transfer coefficients h and k_g are unknown functions of the flow rate. Empirical correlations which are used to evaluate them are related to Nusselt and Sherwood numbers. Gunn [10] proposed the following correlations:

for $0.35 < \varepsilon < 1$ and $Re \leqslant 10^5$

$$N_T = (7 - 10\varepsilon + 5\varepsilon^2)(1 + 0.7\, Re^{0.2}\, m_T^{1/3}) + (1.33 - 2.4\varepsilon + 1.2\varepsilon^2)\, Re^{0.7}\, m_T^{1/3}$$

where

$$N_T = Nu \quad \text{when} \quad m_T = Pr$$

and

$$N_T = Sh \quad \text{when} \quad m_T = Sc.$$

To calculate the effective thermal conductivity of the packed bed, the following correlation is used [11]:

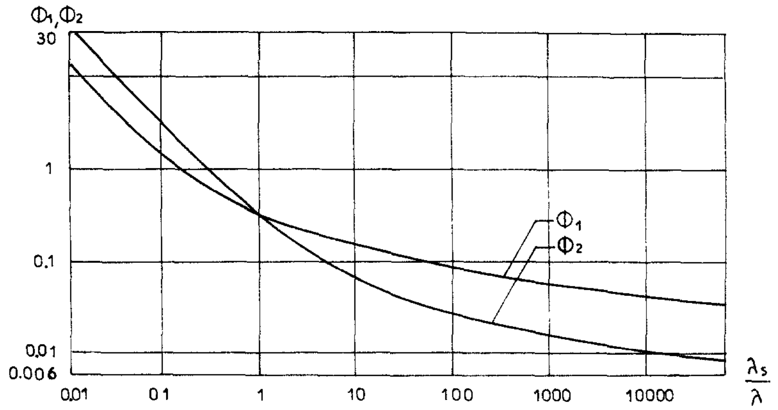

FIG. 2. Coefficients ϕ_1 and ϕ_2 vs λ_s/λ.

$$\frac{\lambda_s^*}{\lambda} = \varepsilon_1 + \frac{(1-\varepsilon_1)\frac{\lambda_s}{\lambda}}{\frac{\phi}{\beta}\frac{\lambda_s}{\lambda} + \left(1 - \frac{\phi}{\beta}\right)}$$

where

$$\varepsilon_1 = \frac{\varepsilon\beta - \phi}{\beta - \phi}.$$

Parameters β and ϕ depend on the geometric characteristics of the porous medium; β is a function of the particles' arrangement and varies between 0.9 and 1—0.9 corresponds to a close arrangement and 1 to a loose one. ϕ is given as

$$\phi = \phi_2 + (\phi_1 - \phi_2)\left(\frac{\varepsilon - 0.26}{0.26}\right) \text{ for } 0.26 < \varepsilon < 0.476$$

$$\phi = \phi_1 \text{ for } \varepsilon > 0.476$$

$$\phi = \phi_2 \text{ for } \varepsilon < 0.26.$$

The values of ϕ_1 and ϕ_2 are shown in Fig. 2 as a function of λ_s/λ.

The reaction studied is the gasification of carbon

$$C + CO_2 \rightleftharpoons 2CO.$$

The enthalpy of this reaction is expressed as [12]

$$\Delta H(T) = 173.14 \times 10^3 + 12.58T - 19.86 \times 10^{-3} T^2 + 5.77 \times 10^{-6} T^3 - 9.07 \times 10^5 T^{-1} \text{ J mol}^{-1}.$$

Boudouard [13] calculated the equilibrium molar fractions at atmospheric pressure by using the relationship

$$-\frac{21\,000}{T} + \log \frac{X_{CO_2 eq}}{(X_{CO\,eq})^2} = -21.4.$$

The other physical properties of the solid and the gas are given in the Appendix.

4. NUMERICAL METHOD

The set of differential equations (9)–(12) and the boundary conditions chosen are solved by using the finite-difference method proposed by Patankar [14], which consists of dividing the reactor into many control volumes the thickness of which is Δx. Those equations are integrated, and their discretization, for T for instance, is of the form

$$a_i T_i = a_{i+1} T_{i+1} + a_{i-1} T_{i-1} + b$$

with a tridiagonal matrix, which allows a gain in time of calculations and place in computer memory. A direct method (Thomas's method [14]) allows the formulation of the final solution to the above set of algebraic equations. The term b, which really expresses heat and mass source terms, may generally be linearized as a function of T_i according to the methods presented in ref. [14].

For calculations, Δx is chosen as 0.04.

5. BEHAVIOUR OF THE MODEL

The numerical solution is made by using the parameters $\theta_0 = 300$ K, $p = 1.013 \times 10^5$ Pa, $C_0 = 41$ mol m^{-3}, $d = 0.003$ m, $\varepsilon = 0.45$, $K = 1200$ m^{-1}, $\lambda_s^* = 0.5$ W m^{-1} K^{-1}.

This has allowed the determination of temperature distributions and gas composition.

Figure 3 shows the temperature distributions for the gas and the solid. It is noted that there are two temperature zones: the first corresponds to the heating of gas by the porous medium exposed to the external radiative source (concentrated solar radiation), and the second to an equilibrium thermal zone between solid and gas.

In the solid, the temperature gradient is very high because the effective thermal conductivity is low.

Figure 4 shows molar fractions of CO and CO_2 profiles in the gas—X_{CO}, X_{CO_2}—as well as equilibrium molar fractions—$X_{CO\,eq}$, $X_{CO_2 eq}$—calculated at the temperature of the reaction, i.e. the surface temperature of the solid particles. The 'direct' reaction zone is located at a small distance from the warm front of the reactor. In this zone, CO is loaded into the gas. In zones neighbouring the warm front (at a distance of a few particle diameters), the entering gas

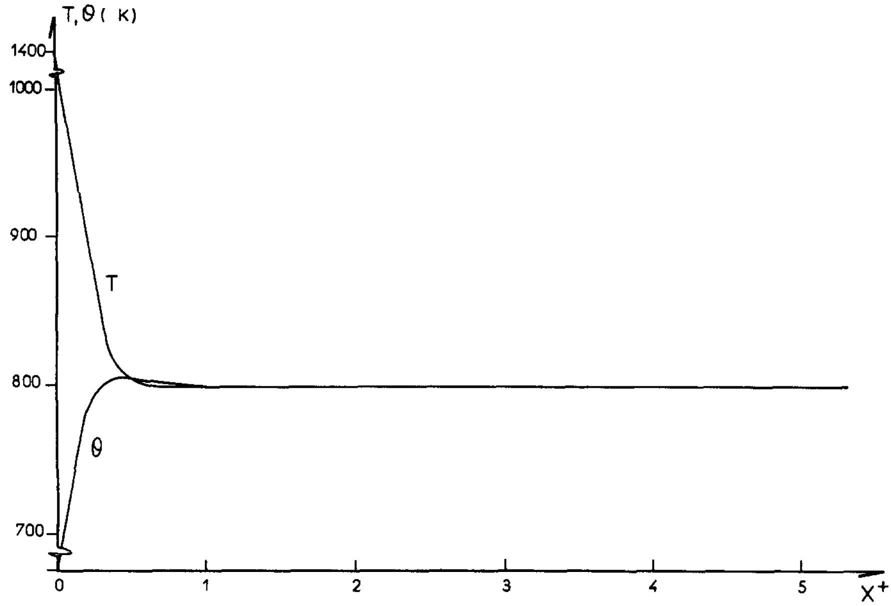

FIG. 3. Temperature distributions for gas and solid along the reactor: $V_0 = 0.06$ m s^{-1}, $T_0 = 1400$ K, $L^+ = 16$.

has a concentration of CO that becomes greater than the equilibrium concentration. The reverse reaction

$$2\,CO \rightarrow C + CO_2$$

adjusts the equilibrium concentration, but this reaction has a null rate in the absence of catalysers in the temperature range considered [15]. This is the reason why the temperature distribution obtained beyond the 'direct' reaction zone is horizontal.

The advancement degree of the reaction (equal to the conversion factor of the reactant, CO_2) is defined as the ratio of CO_2 moles consumed at a distance X^+ into the reactor to the number of moles entering at $X^+ = 0$ in order to characterize the behaviour of the formation of the gas during the reaction and along the reactor

$$X = \frac{C_0 - C^+}{C_0}$$

where

$$C^+ = \frac{\rho C}{M_{CO_2}}.$$

Its behaviour is shown in Fig. 5.

As for the behaviour of the speed of the packed bed, this is shown in Fig. 6.

5.1. *Conduction–radiation interaction*

If conduction transfers are characterized by a conductivity λ_s^*, radiative transfers may also be charac-

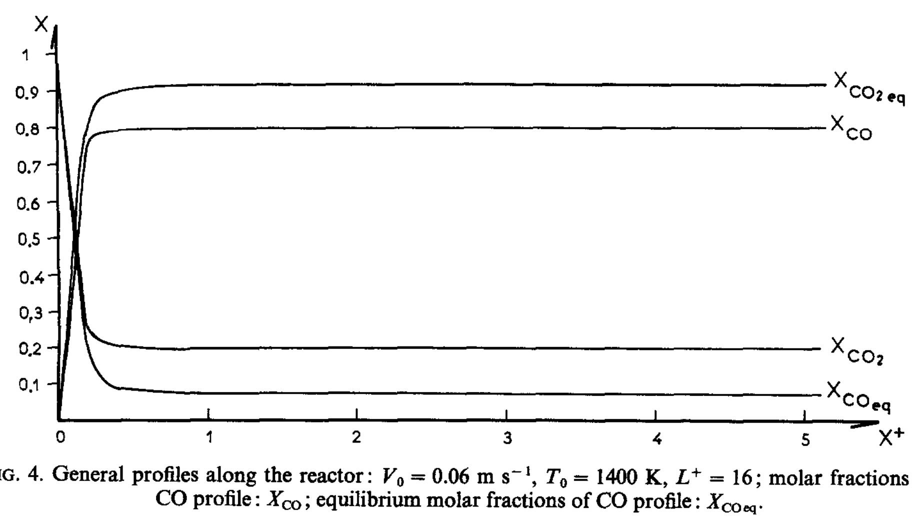

FIG. 4. General profiles along the reactor: $V_0 = 0.06$ m s^{-1}, $T_0 = 1400$ K, $L^+ = 16$; molar fractions of CO profile: X_{CO}; equilibrium molar fractions of CO profile: $X_{CO_{eq}}$.

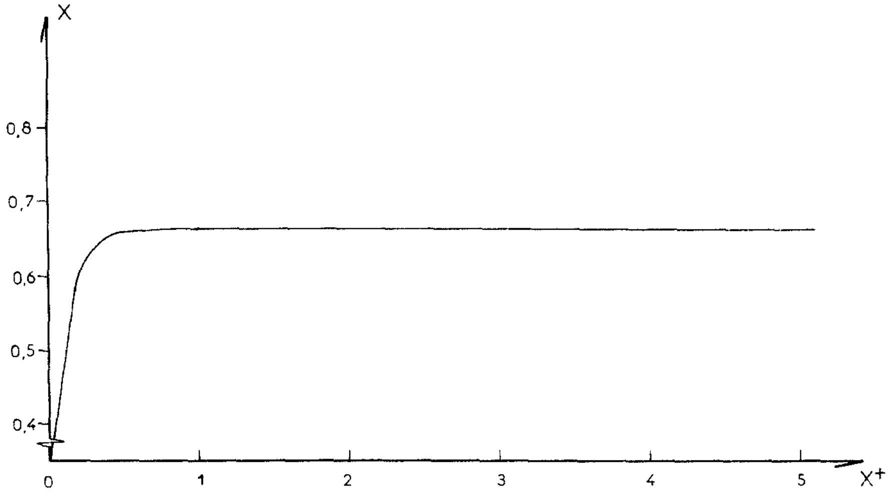

FIG. 5. Degree of advancement of reaction profile: $V_0 = 0.06$ m s^{-1}, $T_0 = 1400$ K, $L^+ = 16$.

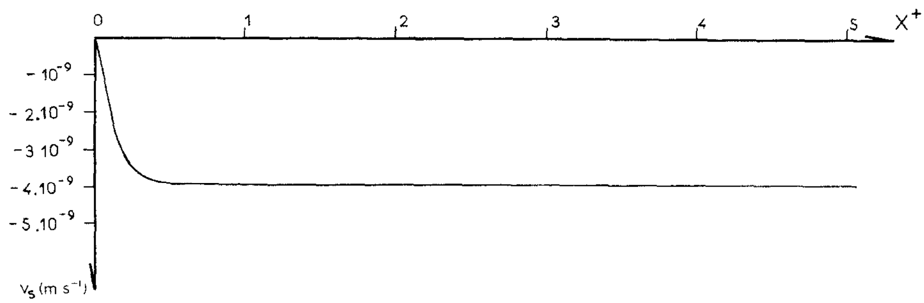

FIG. 6. Velocity of solid profile along the reactor: $V_0 = 0.06$ m s^{-1}, $T_0 = 1400$ K, $L^+ = 16$.

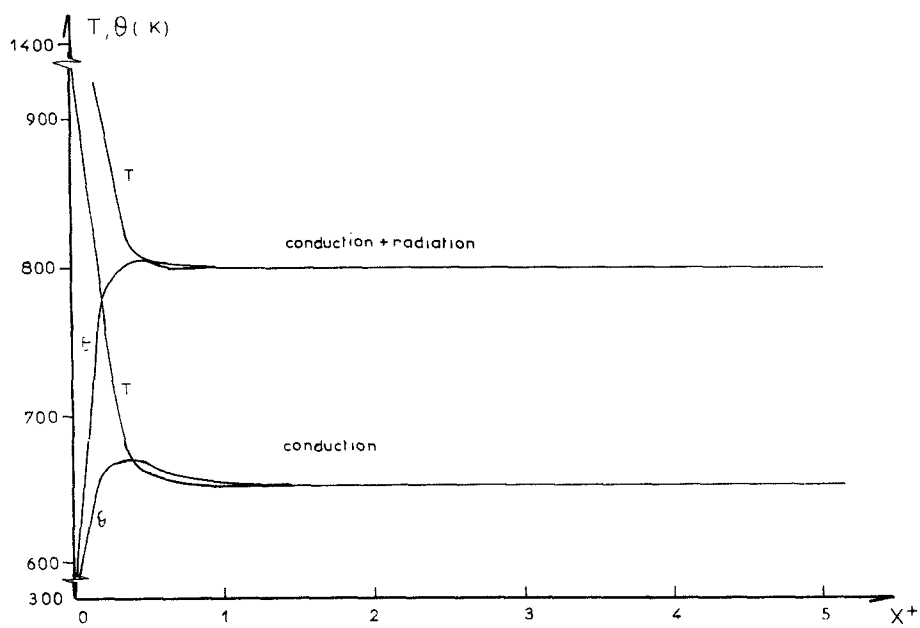

FIG. 7. Effect of the radiative transfer on the temperature distributions: $V_0 = 0.06$ m s^{-1}, $T_0 = 1400$ K, $L^+ = 16$.

terized by a radiative conductivity

$$\lambda_r = \frac{16\sigma T^3}{3K}$$

where K (m^{-1}) is the extinction coefficient per unit medium volume. The interaction between these modes of transfer is evaluated by defining a parameter that is a function of the two conductivities, expressed as [16]

$$N = \frac{4}{3}\frac{\lambda_s^*}{\lambda_r}$$

and known as the Stark number; a value of $N = 1.66$ is found when the average control parameters are $v_0 = 0.004\ m\ s^{-1}$, $d = 0.003$ m, $T_0 = 1100$ K, $\lambda_s^* = 0.5$ W m^{-1} K^{-1} and $K = 1000\ m^{-1}$.

Doornink and Hering [17] showed that for $N < 5$, radiation heat transfer compared to conduction cannot be neglected. This has required the coupling of these two energy exchange modes in the current model.

Shown in Figs. 7 and 8 are the temperature and advancement degree profiles along the reactor in the case of pure conduction (the term $(\partial q_r/\partial x)$ is equal to zero in the solid energy equation) and those given by the model.

It is noted that the temperatures and the advancement degree obtained by the model are higher than those given by pure conduction.

The influence of effective thermal conductivity λ_s^* and of extinction coefficient K on the advancement degree is shown in Figs. 9 and 10.

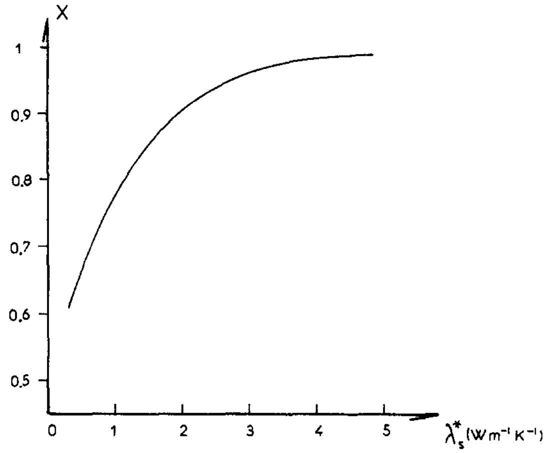

FIG. 9. Effect of the effective conductivity on the degree of advancement of reaction: $V_0 = 0.06$ m s^{-1}, $T_0 = 1400$ K, $L^+ = 16$.

5.2. *Effect of control parameters*

The control parameters chosen are: the warm surface temperature (exposed to incident radiation in $X^+ = 0$) T_0, the flow rate of entering gas in the reactor v_0 and the solid particle diameter d.

An increase in the first parameter increases the advancement degree of the reaction, as is shown in Fig. 11 by the T_0 distribution for different values of flow rate.

An increase in the flow rate leads to a decrease in temperatures and transformation rate, and the effect of v_0 on the latter is graphically represented in Fig. 12.

A decrease in the particle diameter has the effect of increasing the contact surface rate A and therefore of increasing temperatures and transformation rates; see Fig. 13.

The thermochemical efficiency η is defined as the

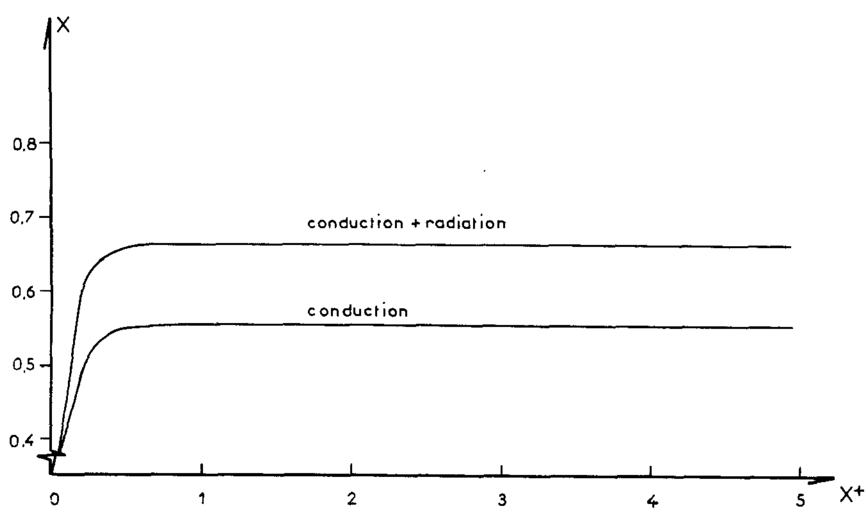

FIG. 8. Effect of the radiative transfer on the degree of advancement of reaction: $V_0 = 0.06$ m s^{-1}, $T_0 = 1400$ K, $L^+ = 16$.

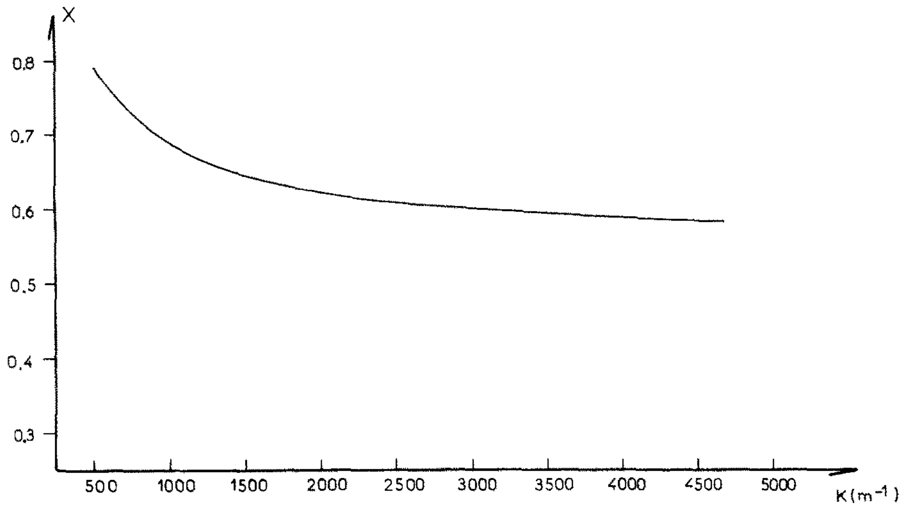

FIG. 10. Effect of the extinction coefficient on the degree of advancement of reaction: $V_0 = 0.06$ m s^{-1}, $T_0 = 1400$ K, $L^+ = 16$.

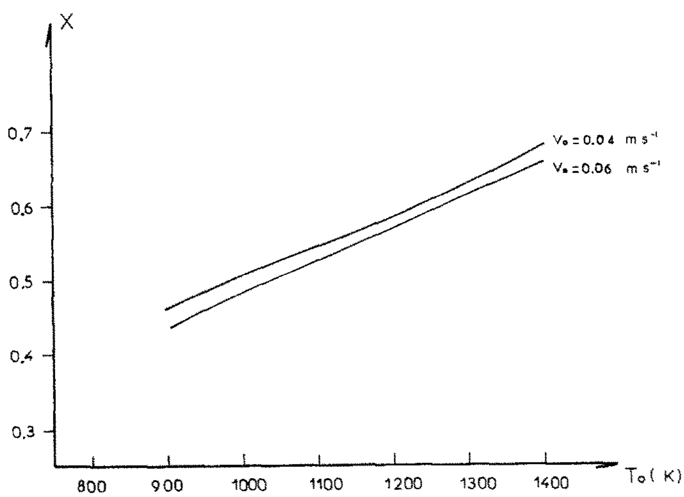

FIG. 11. Effect of the temperature of the warm surface on the degree of advancement of reaction for different velocities of the gas at the entry of the packed bed: $L^+ = 16$.

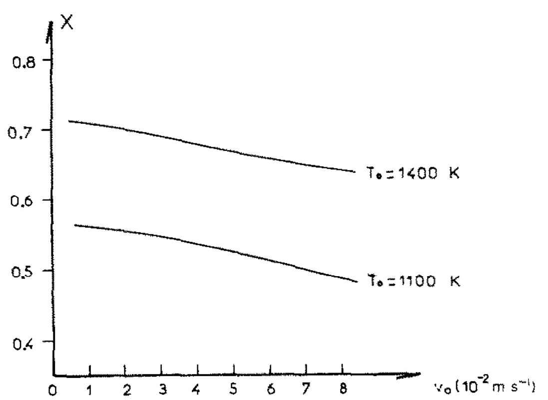

FIG. 12. Effect of the velocity of the gas at the entry of the packed bed on the degree of advancement of reaction for different temperatures of the warm surface: $L^+ = 16$.

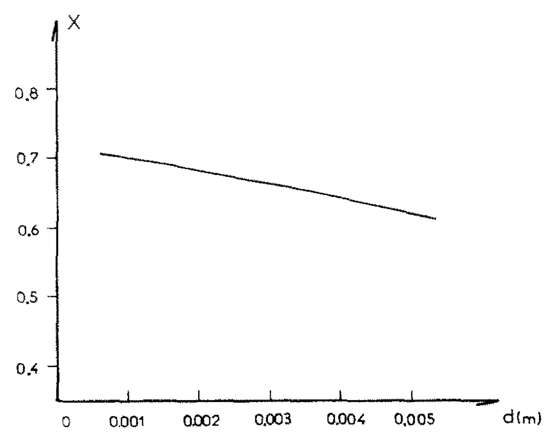

FIG. 13. Effect of the particle diameter on the degree of advancement of reaction: $V_0 = 0.06$ m s^{-1}, $T_0 = 1400$ K, $L^+ = 16$.

ratio of the variation of density flux of gas chemical enthalpy per unit surface area in the reactor to the incident radiative density flux

$$\eta = \left(\frac{\Delta H_p - \Delta H_F}{\Delta H_s}\right) \times 100 = \frac{H_L}{\phi_i}$$

where H_L is a function of overall advancement degree of the reaction at the exit of the gas, of v_0 and of the difference of formation enthalpies of CO and CO_2, and is expressed as

$$H_L = v_0 X_L C_0 [2\Delta H_f^0(CO) - \Delta H_f^0(CO_2)].$$

Hence

$$\eta = \frac{v_0 X_L C_0 [2\Delta H_f^0(CO) - \Delta H_f^0(CO_2)]}{\phi_i}.$$

The external incident radiation density ϕ_i may be calculated by making a thermal balance at the warm surface ($X^+ = 0$), where heat convection is neglected, by using the expression

$$\alpha_g \phi_i = -\lambda_s^* \left(\frac{\partial T}{\partial x}\right)_{x=0} + \varepsilon_g \sigma (T_0^4 - \theta_a^4)$$

where α_g is the overall absorptivity and ε_g the overall emissivity.

The value of ε_g is given by Borodulya *et al.* [18] as

$$\varepsilon_g = \varepsilon_p^{0.485}$$

which is valid when the porosity is about 0.4.

A value of $\eta = 27\%$ is obtained for $v_0 = 0.04\ \mathrm{m\ s^{-1}}$, $T_0 = 1400$ K, $d = 0.003$ m, $K = 1200\ \mathrm{m^{-1}}$, $\lambda_s^* = 0.3\ \mathrm{W\ m^{-1}\ K^{-1}}$, $\varepsilon_p = 0.8$, $\rho_s = 1.4\ \mathrm{kg\ m^{-3}}$ and $\phi_i = 520\ \mathrm{kW\ m^{-2}}$.

Infra-red emission and reflection loss on the exposed surface of the reactor have been estimated to be 37%, and those by sensible heat acquired by the gas to be 7%.

Another characteristic quantity of this reactor, the specific productivity, is defined as

$$P_S = (1-\varepsilon)\rho_S V_{SL}.$$

The value of P_S is found to be equal to 165 kg $\mathrm{h^{-1}\ m^{-2}}$ of C for the conditions defined above.

5.3. *Comparison with experimental results*

The results of the model are compared with experimental values published in ref. [6]. Table 1 shows that satisfactory agreement is found between theoretical and experimental results for temperatures of 950–1200°C and flow rates of 1–8 l $\mathrm{min^{-1}}$ for the following values of the parameters: $d = 0.32$ cm, $\varepsilon = 0.45$, $C_0 = 33.84$ mol $\mathrm{m^{-3}}$, $\theta_0 = 300$ K, $\lambda_s^* = 0.3$ W $\mathrm{m^{-1}\ K^{-1}}$, $k = 1200\ \mathrm{m^{-1}}$, $L = 12$ cm, $D_0 = 4.7$ cm and $p = 84\,000$ Pa.

Table 1. Comparison of model results and experimental results

F_{CO_2} (l $\mathrm{min^{-1}}$)	$T_{0\,cal}$ (°C)	$T_{0\,meas}$ (°C)	X_{cal}	X_{meas}
2	1127	1129	0.84	0.84
3.3	1067	1065	0.79	0.80
3.3	1087	1090	0.80	0.81
4	1087	1083	0.82	0.81
4	1127	1129	0.83	0.83
6	947	1027	0.62	0.67
8.2	987	988	0.55	0.68

6. CONCLUSION

A theoretical model of a chemical moving packed bed reactor for gasifying carbon by using an external radiative heat source and with a mass transport control has been presented. It permits the determination of gas and solid temperature distributions and concentration distributions in the gas along the reactor as functions of various parameters, among which are those of control (gas flow rate, warm surface temperature, particle diameter). The effect of these parameters on the degree of advancement of the reaction is also studied.

Comparison of model results with those from experiments published in ref. [6] gives satisfactory agreement.

REFERENCES

1. D. W. Gregg, R. W. Taylor, J. H. Campbell, J. R. Taylor and A. Cotton, Solar gasification of coal activated carbon, coke and coal and biomass mixture, *Sol. Energy* **25**, 353–364 (1980).
2. D. W. Gregg, W. R. Aiman, H. H. Otsuki and C. B. Thorsness, Solar coal gasification, *Sol. Energy* **24**, 313–321 (1980)
3. W. R. Aiman, C. B. Thorsness and D. W. Gregg, Solar coal gasification: plant design and economics, UCRL Preprint 84610, Lawrence Livermore Laboratory, Livermore, California (1981).
4. R. W. Taylor, R. Berjoan and J. P. Coutures, Solar gasification of carbonaceous materials, *Sol. Energy* **30**, 513–525 (1983).
5. M. C. Quelard, Contribution à la modélisation d'un gazogène à front chaud solaire et lit mobile poreux appliqué à la gazéification de produits carbonés. Thèse de D.I., I.N.P. Toulouse (1983).
6. A. Belghit, Etude théorique et expérimentale d'un gazéifieur solaire de matières carbonées en lit poreux mobile. Thèse de Doctorat, Université de Perpignan (1986).
7. J. Szekely, J. W. Evans and Hong Yong Sohn, *Gas–Solid Reactions*. Academic Press, New York (1976).
8. J. Villermaux, Génie de la réaction chimique. *Technique et Documentation* (Lavoisier) (1982).
9. S. Rosseland, *Theoretical Astrophysics*. Oxford University Press, London (1936).
10. D. J. Gunn, Transfer of heat or mass to particles in fixed and fluidized beds, *Int. J. Heat Mass Transfer* **21**, 467–476 (1978).
11. D. Kunii and J. M. Smith, Heat transfer characteristics of porous rocks, *A.I.Ch.E Jl* **7**, 29–34 (1961).
12. Tables de Barin et Knacke, *Thermo-chemical Properties of Inorganic Substances*. Springer, Berlin (1973).
13. O. Boudouard, *Ann. Chem. Phys.* **24**, 5–85 (1901).

14. V. Patankar Suhas, *Numerical Heat Transfer and Fluid Flow*. McGraw-Hill, London (1978).
15. P. L. Walker Jr., *Chemistry and Physics of Carbon*. Dekker, New York (1969).
16. G. Lauriat, Couplages rayonnement conduction et rayonnement convection dans les milieux semi-transparents. Ecole d'été G.U.T. fascicule 3, Perpignan (1976).
17. D. G. Doornink, R. C. Hering, Transient combined conductive and radiative heat transfer, *Trans. ASME, J. Heat Transfer* 473–478 (November 1972).
18. V. A. Borodulya, V. I. Kovensky and K. E. Makhorin, Radiative heat transfer between a fluidized bed and a surface, *Int. J. Heat Mass Transfer* **26,** 277–287 (1983).
19. R. B. Bird and W. E. Stewart, *Transport Phenomena*. Wiley, New York (1960).
20. W. Reid and H. Sherwood, *The Properties of Gases and Liquids* (2nd Edn). McGraw-Hill, New York (1966).

APPENDIX: PHYSICO-CHEMICAL PARAMETERS

Gas apparent density

$$\rho = \frac{p}{R\theta}\sum_i x_i M_i\,; \quad p = p_0 = p_a = 1.03 \times 10^5 \text{ Pa}$$

where x_i is the molar fraction of the component i of the gas mixture and M_i is its molar density.

Gas heat capacity per unit mass

$$c_p = \sum_i C_i(\theta) c_{pmi}(\theta)$$

where c_{pmi} is the heat capacity per unit of mass of the i component of the gas mixture and C_i is its mass fraction; $c_{pmi} = c_{pi}/M_i$, where the values of c_{pi} are [12]

$$c_{pCO} = 28.38 + 4.1 \times 10^{-3}\theta - 0.46 \times 10^5 \theta^{-2} \text{ J mol}^{-1} \text{ K}^{-1}$$

$$c_{pCO_2} = 44.1 + 9.03 \times 10^{-3}\theta - 8.53 \times 10^5 \theta^{-2} \text{ J mol}^{-1} \text{ K}^{-1}.$$

Gas viscosity [19]

$$\mu = \sum_{i=1}^{2} \frac{x_i \mu_i}{\sum_{j=1}^{2} x_j \phi_{ij}}$$

where x_j is the molar fraction of the component j and ϕ_{ij} is written as

$$\phi_{ij} = \frac{1}{\sqrt{8}}\left[1 + \frac{M_i}{M_j}\right]^{-1/2}\left[1 + \left(\frac{\mu_i}{\mu_j}\right)^{1/2}\left(\frac{M_j}{M_i}\right)^{1/4}\right]^2$$

μ_i and μ_j are the viscosities of components i and j at the temperature θ, given by Sutherland's relationship [20]

$$\mu_i(\theta) = \mu_i(273)\left[\frac{273 + C_i}{\theta + C_i}\right]\left[\frac{\theta}{273}\right]^{2/3}$$

$$\mu_{CO}(273) = 16.6 \times 10^{-6} \text{ N s m}^{-2}; \quad \mu_{CO_2}(273) = 13.83 \times 10^{-6} \text{ N s m}^{-2};$$

$$C_{CO} = 97.93 \text{ K}; \quad C_{CO_2} = 231.28 \text{ K}$$

Thermal conductivity of the gas

$$\lambda = \sum_{i=1}^{2} \frac{x_i \lambda_i}{\sum_{j=1}^{2} x_j \phi_{ij}}$$

where λ_i is given by Sutherland's relationship

$$\lambda_i(\theta) = \lambda_i(273)\left[\frac{273 + C_i}{\theta + C_i}\right]\left[\frac{\theta}{273}\right]^{2/3}$$

with $\lambda_{CO}(273) = 0.022$ W m^{-1} K^{-1}, $\lambda_{CO_2}(273) = 0.0144$ W m^{-1} K^{-1}, $C_{CO} = 515.8$ K and $C_{CO_2} = 1334.7$ K.

Diffusion coefficient

Fuller *et al.*'s relationship [20] gives

$$D = D_{ij} = 10^{-7}\frac{\theta^{1.75}}{p[V_i^{1/3} + V_j^{1/3}]^2}\left[\frac{1}{M_i} + \frac{1}{M_j}\right]^{1/2}$$

where V_i and V_j are the diffusion volumes of i and j. Hence $V_{CO} = 18.9 \times 10^{-6}$ m^3; $V_{CO_2} = 26.9 \times 10^{-6}$ m^3; $p = 1$ atm.

Heat capacity of the solid

The heat capacity per unit of mass of the solid is given by

$$c_{ps} = c_{pmc} M_C^{-1}$$

where c_{pmc} is the molar heat capacity of the solid the molar density of which is M_C. Hence

$$c_{pmc} = 0.109 + 39.04 \times 10^{-3} T - 1.48 \times 10^5 T^{-2} - 17.37 \times 10^{-6} T^2 \text{ J mol}^{-1} \text{ K}^{-1}.$$

ETUDE DU TRANSFERT DE CHALEUR ET DE MASSE DANS UN REACTEUR CHIMIQUE A LIT MOBILE POUR LA GAZEIFICATION DU CHARBON EN UTILISANT UNE SOURCE RADIANTE EXTERNE

Résumé—On propose un modèle théorique du réacteur chimique à lit mouvant pour la gazéification du charbon avec du CO_2, en utilisant une source radiante externe (rayonnement solaire concentré). Il permet la détermination du profil de température du gaz et du solide, des profils de concentration dans le gaz en fonction des paramètres opératoires: débit de gaz, température de la surface chaude, diamètre des particules. La comparaison des résultats du modèle avec l'expérience donne un accord satisfaisant.

UNTERSUCHUNG DES WÄRME- UND STOFFTRANSPORTS IN EINEM CHEMISCHEN FLIESSBETT-REAKTOR ZUR KOHLEVERGASUNG BEI VERWENDUNG EINER EXTERNEN STRAHLUNGSQUELLE

Zusammenfassung—Es wird ein theoretisches Modell eines Fließbett-Reaktors zur Kohlevergasung mit CO_2 bei Verwendung einer externen Strahlungsquelle (konzentrierte Sonnenstrahlung) vorgeschlagen. Es ermöglicht die Bestimmung der Temperaturprofile im Gas und im Feststoff als Funktion folgender Parameter: Gasvolumenstrom, Oberflächentemperatur und Partikeldurchmesser. Vergleiche zwischen Modell und Experiment ergeben eine zufriedenstellende Übereinstimmung der Ergebnisse.

ИССЛЕДОВАНИЕ ТЕПЛО- И МАССОПЕРЕНОСА В ХИМИЧЕСКОМ РЕАКТОРЕ С ДВИЖУЩИМСЯ СЛОЕМ ДЛЯ ГАЗИФИКАЦИИ УГЛЯ ПРИ ИСПОЛЬЗОВАНИИ ВНЕШНЕГО ИСТОЧНИКА ИЗЛУЧЕНИЯ

Аннотация—Предложена теоретическая модель химического реактора с движущимся слоем для газификации угля при наличии углекислого газа и внешнего источника излучения (концентрованной солнечной энергии). Данная модель позволяет определить профиль температур для газа и твердого вещества и профиль концентраций газа как функцию контрольных параметров: расхода газа, температуры нагретой поверхности, диаметра частиц. Результаты удовлетворительно согласуются с экспериментом.